frontiers | Frontiers in Materials

TYPE Original Research
PUBLISHED 06 December 2023
DOI 10.3389/fmats.2023.1280543

OPEN ACCESS

EDITED BY
Han Eol Lee,
Jeonbuk National University, Republic of Korea

REVIEWED BY
Sandeep G. Surya,
Dyson, United Kingdom
Lakshmi Narayanan Mosur Saravana Murthy,
Intel, United States

*CORRESPONDENCE
Leszek A. Majewski,
leszek.majewski@manchester.ac.uk
Abdou Karim Diallo,
abdou-karim.diallo@ugb.edu.sn

†PRESENT ADDRESS
Sheida Faraji, Electronics and Communication Engineering Department, Istanbul Technical University, Ayazaga Campus, Maslak, Istanbul, Türkiye; Aybüke Tavasli, Department of Materials Science and Engineering, Istanbul Technical University, Ayazaga Campus, Maslak, Istanbul, Türkiye

RECEIVED 20 August 2023
ACCEPTED 13 November 2023
PUBLISHED 06 December 2023

CITATION
Faraji S, Tall A, Mohammadian N, Seck M, Saadi M, Tavasli A, Erouel M, Khirouni K, Diallo AK and Majewski LA (2023), Towards sustainable, solution-processed organic field-effect transistors using cashew gum as the gate dielectric. *Front. Mater.* 10:1280543. doi: 10.3389/fmats.2023.1280543

Towards sustainable, solution-processed organic field-effect transistors using cashew gum as the gate dielectric

Sheida Faraji[1,2†], Abdoulaye Tall[3], Navid Mohammadian[1], Mané Seck[3], Meriem Saadi[4], Aybüke Tavasli[2†], Mohsen Erouel[4], Kamel Khirouni[4], Abdou Karim Diallo[3]* and Leszek A. Majewski[1]*

[1]Department of Electrical and Electronic Engineering, University of Manchester, Manchester, United Kingdom, [2]Nanotechnology Research Centre (ITUnano), Maslak, Advanced Technologies Centre, Istanbul, Türkiye, [3]Département de Physique Appliquée, UFR de Sciences Appliquées et de Technologie, Université Gaston Berger, Saint-Louis, Senegal, [4]Laboratoire de Physique des Matériaux et des Nanomatériaux Appliquée à l'Environnement, Faculté des Sciences de Gabès, Université de Gabès, Gabès, Tunisia

To realize low-cost, environmentally friendly electronic devices and circuits, there is currently a strong trend to explore plant-based dielectric materials because they can be responsibly sourced from agricultural or forest vegetation, are generally water-soluble, and possess good electrical insulator properties. In this contribution, organic field-effect transistors (OFETs) using a biopolymer dielectric obtained from exudates of *Anacardium occidentale* Linn. trees, namely, cashew gum (CG), are reported. To characterise the physical and dielectric properties of the gum, thin films and metal-insulator-metal (MIM) capacitors were prepared and characterized. To evaluate the material's performance in OFETs, bottom-gate top-contact (BGTC) p-channel poly [3,6-di(2-thien-5-yl)-2,5-di(2-octyldodecyl)-pyrrolo (3,4-c)pyrrole-1,4-dione) thieno (3,2-b) thiophene]:polymethyl methacrylate (DPPTTT:PMMA) transistors were engineered and studied. The fabricated MIM capacitors display a comparatively high areal capacitance of 260 nF/cm^2 at 1 kHz for 130 nm thick films. As a result, the solution-processed DPPTTT:PMMA OFETs favourably operate at 3 V with the average saturation field-effect mobility equal to 0.20 cm^2/Vs., threshold voltage around −1.4 V, subthreshold swing in the region of 250 mV/dec, and ON/OFF current ratio well above 10^3. As such, cashew gum emerges as a promising dielectric for sustainable manufacturing of solution-processed organic FETs.

KEYWORDS

organic field-effect transistor (OFET), biopolymer dielectric, cashew gum, solution processing, sustainable electronic devices

1 Introduction

During the past few decades, the evolution of microelectronic components, and particularly field-effect transistors (FETs), has mainly been driven by the innovations in inorganic electronic materials. Today, with many new challenges such as engineering of skin wearable devices and sensors, as well as environmental concerns relating to the electronic waste (e-waste), there is an increased interest in the development of FETs that use organic semiconductors, so-called OFETs, because they can be inexpensively fabricated using

environmentally friendly, solution-based techniques and can employ biocompatible and/or biodegradable materials (Irimia-Vladu et al., 2010a). Commonly, the research on OFETs focuses on the synthesis of high carrier mobility, air-stable organic semiconductors (Hu et al., 2021). Here, however, we concentrate on another key element of organic FETs, namely, the dielectric layer that separates the transistor active material and the gate electrode. Since the physical and electrical properties of this layer strongly influence the operation and performance of OFETs, it is paramount to employ appropriate materials (Paterson et al., 2019).

To date, many studies have been conducted on man-made and naturally occurring organic and inorganic gate dielectrics for OFETs (Chiong et al., 2021; Cenci et al., 2022). In particular, polymer insulators have been extensively studied owing to their room temperature solution-based processing, good mechanical and electric insulation properties, as well as high compatibility with a wide range of rigid and flexible substrates. Recently, low threshold voltage organic FETs operating with gate voltages $|V_G| \leq 5$ V that use low-k and high-k polymers, as well as low-k/high-k polymer bi- and multilayers as the gate dielectric have been reported (Nketia-Yawson and Noh, 2018; Xu et al., 2023). However, the majority of the researched solution-deposited materials have been synthetic polymers, and so far, there is a relatively small number of studies reporting low-voltage operating OFETs using naturally occurring biopolymer dielectrics (Irimia-Vladu, 2014; Wang et al., 2019).

Regarding biopolymer dielectrics, electric insulators of plant origin have lately attracted increased attention of material and device engineers because they can be readily processed into thin films from aqueous solutions in ambient conditions and generally display good dielectric properties. Indeed, several examples of low-voltage operating OFETs using a wide range of plant- and tree-based materials as the gate insulator including almond, arabic, and khaya gums, have just been reported (Ivić et al., 2022; D'Orsi et al., 2022; Seck et al., 2020a; Seck et al., 2020b; Tall et al., 2022). Here, organic field-effect transistors using an alternative gum, i.e., cashew gum (CG), that operate with $|V_G| \leq 3$ V are demonstrated.

CG is a polysaccharide complex obtained from exudates of *Anacardium occidentale* Linn. trees, commonly known as cashew, that are native to North-eastern Brazil and South-eastern Venezuela but nowadays also grow in Sub-Saharan Africa (e.g., Ivory Coast, Nigeria, Senegal, etc.) and South Asia (e.g., India, Vietnam, Philippines, etc.). In terms of its chemical structure, cashew gum is composed of a main β-galactose (1→3) chain with branches of β-galactose (1→6) and terminal residues of glucuronic acid, arabinose, rhamnose, 4-O-methylglucuronic acid, xylose, glucose, and mannose (Murthy, 2022). As such, its composition is significantly different from other natural gums that were previously applied in OFETs. Furthermore, CG is much more readily available, and thus much cheaper than, for example, almond or khaya gums. In Brazil alone, the average production of cashew gum is 700 g per tree per year with a potential annual production of around 50,000 tons (Ribeirod et al., 2016). As a result, CG has become the material of choice for many important industries including food, pharmaceutical and biomedical commerce (Dendena and Corsi, 2014; Hasnain and Nayak, 2019; Vázquez-González et al., 2021). In this contribution, we show that cashew gum can also be used to engineer well-operating electronic devices such as organic field-effect transistors which might pave the way for the use of the material in the manufacturing of sustainable electronic devices and chemical sensors.

Before the fabrication of the transistors, several material characterization tools were used to analyse the physical and electrical properties of the gum. The X-ray diffraction (XRD) measurements of the CG powder showed that the material is largely amorphous. The energy dispersive X-ray fluorescence (EDXRF) characterization revealed that the gum contains many mineral elements which is in a strong agreement with previously published reports (Gyedu-Akoto et al., 2008). Furthermore, surface morphology studies of CG powder using field emission scanning electron microscopy (FESEM) and thin films using atomic force microscopy (AFM) unveiled that the surface of cashew gum is relatively rough and irregular. As it is the case with other polysaccharide complexes, contact angle measurements confirmed that the surface of CG is hydrophilic (Phillips and Williams, 2020).

To investigate the dielectric properties of cashew gum thin films, metal-insulator-metal (MIM) capacitors were fabricated and characterized. It has been found that the devices display a relatively high areal capacitance C_i of (260 ± 28) nF/cm at 1 kHz for (130 ± 20) thick films ($k \approx 38 \pm 2$). As such, the fabricated poly (3,6-di (2-thien-5-yl)-2,5-di (2-octyldodecyl)-pyrrolo [3,4-c] pyrrole-1,4-dione) thieno [3,2-b] thiophene):polymethyl methacrylate (DPPTTT:PMMA) OFETs favourably operate at the gate voltages $|V_{GS}| \leq 3$ V with a saturation field-effect mobility $\mu_{sat} = (0.20 \pm 0.05)$ cm^2/Vs., threshold voltage $V_{th} = -(1.4 \pm 0.1)$ V, subthreshold swing SS = (250 ± 10) mV/dec, and ON/OFF current ratio $I_{ON/OFF} \geq 10^3$. The gate leakage current at $V_{GS} = -3$ V has been measured in the region of 10^{-8} A that is minimum two orders of magnitude lower than the drain-source current. This transistor performance is comparable with or indeed better than the previously reported solution-processed OFETs using plant-based biopolymers as the gate dielectric (Ivić et al., 2022; D'Orsi et al., 2022). Consequently, cashew gum emerges as an attractive alternative dielectric material for sustainable engineering of solution-processed OFETs.

2 Materials and methods

2.1 Preparation and purification of the material powder

First, the material was converted from a hardened sap into powder with an agate mortar and pestle, and then sieved. After that, the gum was washed for 30 min in cyclohexane (Sigma-Aldrich, UK), filtered through a filter paper, and dried for 45 min in ambient conditions. To finish, the dry gum was washed in ethanol (Sigma-Aldrich, UK). The above-described purification process was repeated twice before the material was used for further investigations.

2.2 Physical characterization of the material powder and thin films

To examine the physical properties of the cashew gum powder and thin films, X-ray diffraction (XRD), energy dispersive X-ray

fluorescence (EDXRF), field-emission scanning electron microscope (FESEM), atomic force microscope (AFM), and droplet contact angle (DCA) measurements were performed. The XRD study of the CG powder was done with a Philips PW1840 diffractometer using a copper anode with X-ray wavelength λ = 1.54060 Å and X-ray tube voltage and current equal to 40 kV and 25 mA, respectively. The angular scanning was carried out from 10° to 80° with step of 0.02° using the diffractometer software. To determine the mineral elements in the cashew gum powder, initially the powder was compressed using 10-ton hydraulic press to obtain pellets and then the material was characterised with a portable EDXRF spectrometer (Niton XL3t900s Gold Air) operating at 50 kV and 40 µA. To form thin films, a 2.5 wt% aqueous solution of CG was prepared by dissolving the gum powder in high purity deionised water at room temperature. To assure that the material was fully dissolved, the solution was stirred for 24 h. Before the processing, the CG solution was filtered through a 0.45 µm PTFE membrane filter. The filtered solution was then spin-coated at 3,500 rpm for 2 min onto 1 cm × 1 cm Corning® glass substrates. Finally, the thin films were annealed at 100°C for 30 min in ambient air. The thickness of the obtained thin films was measured with a Bruker Dektak XT Stylus profilometer and was estimated to be (130 ± 20) nm. The surface morphology of the prepared cashew gum thin films was studied using a Zeiss Ultra-plus 55 Field Emission Scanning Electron Microscope (FESEM) operating at 1.0 kV and a non-contact mode Park Systems Atomic Force Microscope (AFM) model XE-100. To study the wetting properties of the cashew gum surface, contact angle (CA) measurements were carried out using an optical contact angle (OCA) data physics system equipped with a high-resolution CCD camera video measuring system.

2.3 Fabrication and characterization of MIM capacitors

First, 100 nm thick 99.99% pure bottom Al electrodes were thermally evaporated onto 1 cm × 1 cm Corning® glass substrates through a shadow mask. Then, the filtered CG solution was spin-coated at 3,500 rpm for 2 min onto the samples and the obtained thin films were annealed at 100°C for 30 min in ambient conditions. The fabrication of capacitors was completed by evaporation of 100 nm thick 99.99% pure top Al contacts. After that, capacitance per unit area (C_i) and dissipation factor (DF) versus frequency (f) were measured in ambient conditions with an Agilent E4980A LCR meter from 100 Hz to 1 MHz, respectively. To finish the characterization of capacitors, capacitance per unit area (C_i) against the applied voltage (V) was measured at 1 kHz using the same LCR meter.

2.4 Fabrication and characterization of organic transistors

To fabricate OFETs, first the filtered CG solution was spin-cast at 3,500 rpm for 2 min onto 1 cm × 1 cm Corning® glass substrates with the pre-fabricated 100 nm thick 99.99% pure Al gate electrodes and then the samples were annealed at 100°C for 30 min in air. Subsequently, the organic semiconductor/insulator polymer blend

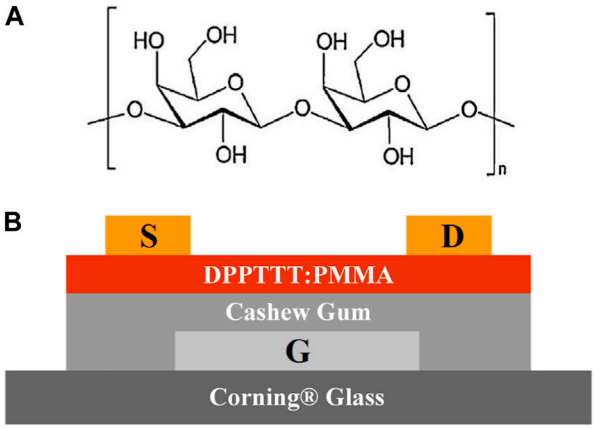

FIGURE 1
(A) The simplified chemical structure of cashew gum showing the galactose backbone. **(B)** Cross section of the fabricated DPPTTT: PMMA OFETs. The gate (G) terminal was made of 99.99% Al, and the source (S) and drain (D) electrodes were made of 99.999% Au.

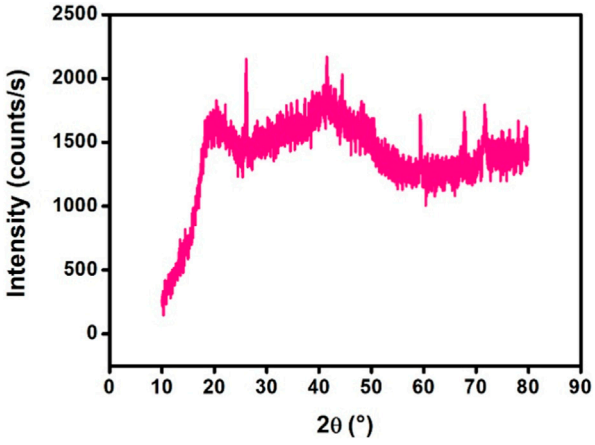

FIGURE 2
A representative XRD diffractogram of the prepared cashew gum powder.

active layer was prepared by dissolving DPPTTT (Luminosyn™ DPP-DTT, Ossila Ltd., UK) and PMMA (Sigma-Aldrich, UK) in 1,2-dichlorobenzene (Sigma-Aldrich, UK) at a solution volume ratio of 7:3. Then, the DPPTTT:PMMA solution was spin-cast at 2,000 rpm for 2 min onto the pre-prepared CG films and the samples were annealed at 90°C for 2 h in nitrogen. Lastly, 50 nm of 99.999% pure Au was evaporated through a shadow mask to form the source and drain electrodes. The structure of the fabricated bottom-gate top-contact (BGTC) OFETs is shown in Figure 1B. The channel length (L) and width (W) of each transistor were 30 and 1,000 µm, respectively. The electrical characterization of the DPPTTT:PMMA OFETs was performed using an Agilent E5270B Precision IV Analyzer with Karl Süss PH100 micromanipulator probes. To evaluate the electrical stability of the fabricated DPPTTT: PMMA OFETs during operation, a constant voltage was applied to

TABLE 1 Major mineral elements found in the prepared cashew gum powder.

CuO (%)	ZnO (%)	CaO (%)	SiO_2 (%)	Fe_2O_3 (%)	P_2O_5 (%)	K_2O_3 (%)	MnO (%)	TiO_2 (%)
70.29	9.69	1.47	13.30	0.12	0.96	0.33	0.07	0.05

TABLE 2 Mineral elements in trace found in the prepared cashew gum powder.

Sr (ppm)	Rb (ppm)	Mo (ppm)	Nb (ppm)	Zr (ppm)	W (ppm)	Cl (ppm)	Cd (ppm)	S (ppm)
16.64	5.38	18.80	22.13	46.15	109.43	84.83	14.62	148.74

the gate electrode for a pre-defined period of time and then forward and backward transfer characteristics were recorded. All electrical characterisations were performed in ambient conditions at 23°C and ~40% RH.

3 Results

3.1 Chemical and physical characterization of cashew gum

Cashew gum was collected from exudates of *Anacardium occidentale* Linn. trees growing in Senegal. As discussed earlier, CG is a complex polysaccharide compound (Murthy, 2022). The simplified chemical structure of cashew gum showing the galactose backbone is presented in Figure 1A and the cross section of the fabricated DPPTTT: PMMA OFETs using CG as the gate insulator in Figure 1B, respectively. Initially, the structural properties of the prepared cashew gum powder were studied using XRD. Figure 2 shows the obtained XRD spectrum. As can be seen, there are no peaks for $2\theta \leq 20^{\circ}$. Interestingly, two strong diffraction peaks are recorded at approximately $2\theta = 26^{\circ}$ and 42°, respectively, which indicates the presence of a crystalline phase. Nevertheless, the overall appearance of the diffractogram suggests that the material is largely amorphous. Indeed, similar XRD diffractograms have been previously reported for cashew and other gums (de Oliveira et al., 2014; Rezaei et al., 2016; Oliveira et al., 2021). Ideally, the gate dielectric layer in OFETs should completely separate the channel of the transistor from the gate electrode and no current should flow through the gate insulator to the gate contact. As such, amorphous dielectric materials are preferred because the presence of a crystalline phase (i.e., grains) may lead to an increased surface roughness of the material, and in consequence, formation of undesired leakage current paths, which significantly contributes to the reduction of the transistor performance (Majewski et al., 2004; Guo et al., 2022).

To determine the elemental composition of the prepared cashew gum powder, energy dispersive X-ray fluorescence (EDXRF) and Fourier Transform Infrared (FTIR) spectroscopy characterizations were carried out. In general, it is very difficult to confirm the presence of chemical elements with low atomic numbers (e.g., carbon) using EDXRF. Hence, EDXRF was used to resolve high atomic number inorganic compounds and FTIR was employed to identify carbon-based compounds (to be reported in detail elsewhere). The contents of the major and minor mineral elements in the examined cashew gum powder obtained from the EDXRF measurements are shown in Tables 1, 2, respectively. The major elements are represented as their corresponding oxides, i.e., CaO, Fe_2O_3, P_2O_5, etc., with a predominance of CuO (70.29%), SiO_2 (13.30%), and ZnO (9.69%). It is worth noting that cashew gum also contains chemical elements such as strontium (Sr), rubidium (Rb), chlorine (Cl), cadmium (Cd), sulphur (S), zirconium (Zr), molybdenum (Mo), niobium (Nb) and tungsten (W) that are present in traces (cf. Table 2). Previously reported studies of the physico-chemical properties of CG and cashew/xanthan gum blends by Guyedu-Akoto *et al.* and Fosu *et al.*, respectively, have also shown the presence of these elements (Gyedu-Akoto et al., 2008; Fosu et al., 2016). However, the chemical composition of CG may greatly differ due to the genotypic differences and age of the trees, as well as plant pathogens, climatic conditions and soil composition (Bedan et al., 2014). Hence, the reported concentration of oxides and chemical elements obtained from EDXRF measurements may vary depending on the source of CG.

Subsequently, the morphology of the cashew gum powder surface was evaluated using FESEM. As shown in Figure 3A, it is clear that the surface of CG is rather non-uniform and irregular. This is due to the presence of small crystallites which may form during the preparation of the powder. Also, since the solubility of gums depends on their molecular weight and the amount of galactose substitution within the chain, not all material might dissolve during the powder preparation (Murthy, 2022).

Following the FESEM assessment, the material was dissolved in high purity deionised water, filtered through a 0.45 µm PTFE filter, and thin films of the gum were prepared. Then, the surface topography of the fabricated films was evaluated using AFM. As can be seen in Figures 3B, C, the prepared films appear to be relatively rough with a root-mean-square (RMS) roughness of around 1.2 nm and a peak-to-valley (PTV) distance of about 10.2 nm. To achieve the best transistor performance, the surface of the gate dielectric in OFETs should be as smooth as possible. This can be accomplished by tailoring the surface of the insulator layer by, for example, using self-assembled monolayers (SAMs) or gas plasma treatment (Seong et al., 2015; Urasinska-Wojcik et al., 2015). However, here we adopted a different approach, namely, we applied a polymer binary blend consisting of DPPTTT and PMMA which after drying forms a semiconductor-insulator double layer. To obtain the semiconductor on the top and the insulator on the bottom using this combination of polymers, the surface of the substrate must be hydrophilic (Qiu et al., 2008; Lee and Park, 2014). To establish whether the surface of cashew gum fulfils this requirement, contact angle measurements were carried out. Figure 4 shows the images of a water droplet on the surface of a CG film at t = 1 s, t = 30 s and t = 60 s. The corresponding contact angles between the gum surface and the water surface were measured to be

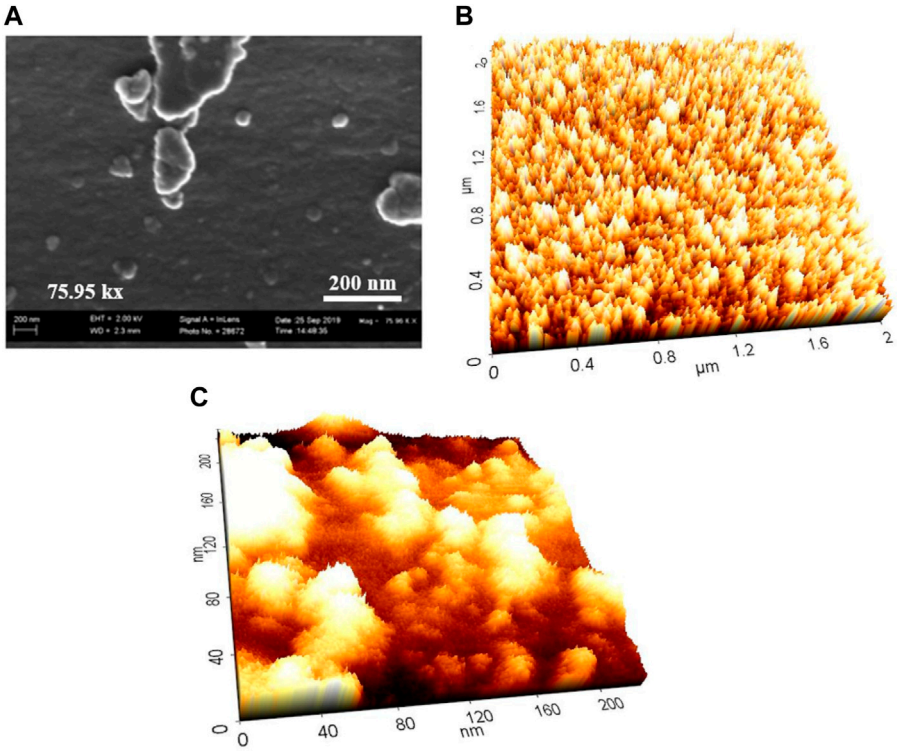

FIGURE 3
(A) A FESEM micrograph of the investigated cashew gum powder. **(B)** 2 μm × 2 μm, and **(C)** 220 nm × 220 nm AFM topography images of the studied cashew gum thin films, respectively.

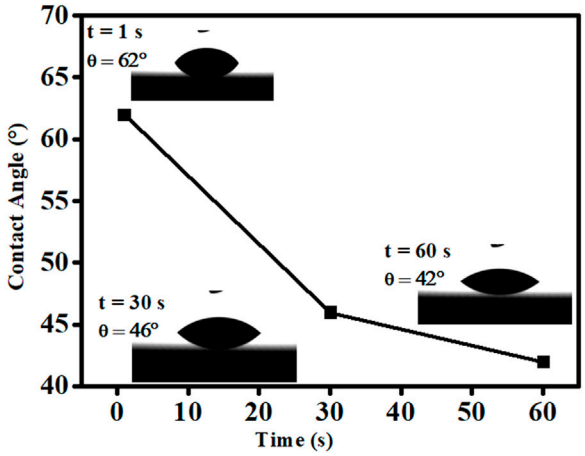

FIGURE 4
Contact angle measurements vs. time showing the evolution of the water droplet shape on the surface of the studied cashew gum film.

$\theta = 62^{\circ}$, $\theta = 46^{\circ}$, and $\theta = 42^{\circ}$, respectively. All these values are smaller than 90° proving that the cashew gum film surface is hydrophilic. Interestingly, the contact angle values decrease from $\theta = 62^{\circ}$ at t = 1 s to $\theta = 42^{\circ}$ at t = 60 s. Such behaviour has been observed in synthetic and biopolymers before and can be attributed to the time-dependent surface reorientation of hydrophilic and hydrophobic groups which occurs upon wetting of polymer surfaces with water (Tretinnikov and Ikada, 1994).

3.2 Characterization of cashew gum-based capacitors

To study the dielectric properties of cashew gum films, MIM capacitors were fabricated. The electrical characterization of the devices was performed using an LCR meter in ambient conditions. Figures 5A, B show the variation of the capacitance per unit area (C_i) and the dissipation factor (DF) as a function of the frequency (f) for 130 nm thick CG films, respectively. It can be clearly seen that C_i gradually decreases from 270 nF cm^{-2} at 100 Hz to 200 nF cm^{-2} at 1 MHz. Ideally, the value of C_i should be independent of f. The lower values of C_i at high f may be due to the dipole polarization in the material. At low frequencies, the dipoles can easily follow the applied electric field, however, when the frequency increases, they have gradually less time to line up in the direction of the field, and consequently, the measured values of C_i decrease. In addition, the higher values of C_i at low f may be due to the interfacial polarization (space charge displacement). At frequencies below 10^4 Hz, extraneous charges originating from impurities and/or irregular geometry in the interfaces of polycrystalline solids are partly mobile and migrate under an applied field causing the extrinsic type of polarization. Such C_i vs. f behaviour has been observed before and is common for most high-k polymer dielectrics (Xia and Zhang, 2018; Kim et al., 2021). Correspondingly, the calculated value of the dielectric constant (k) for 130 nm thick CG films quickly decreases from about

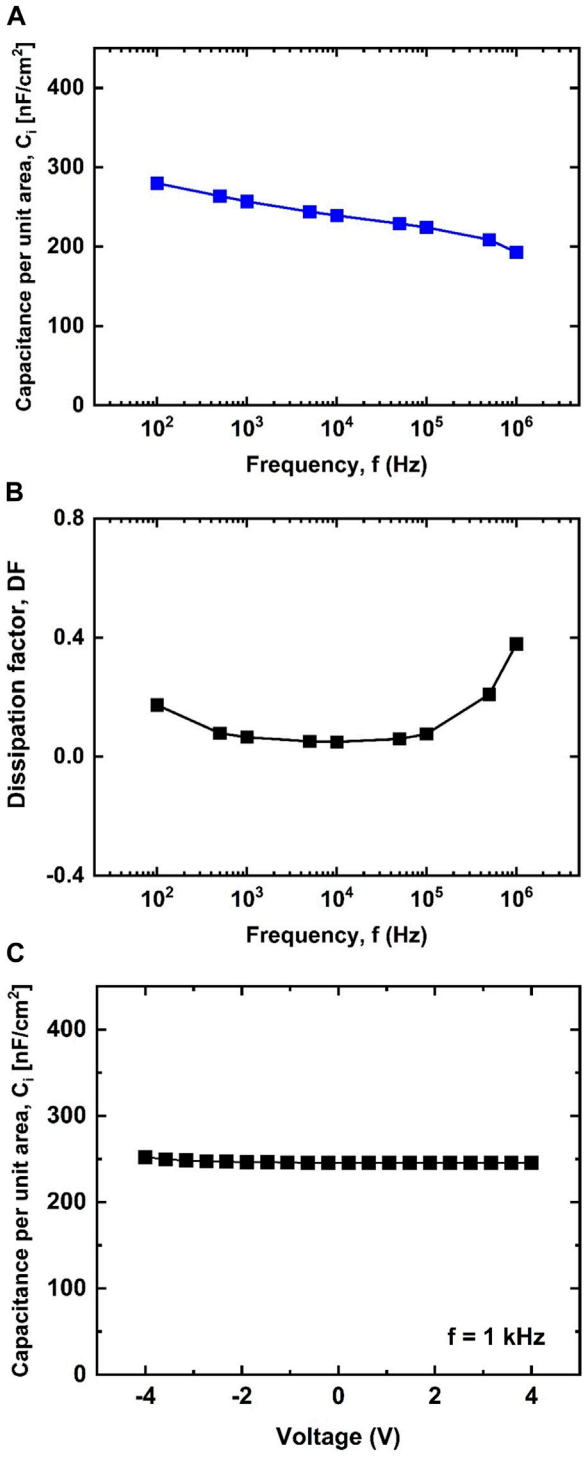

FIGURE 5
(A) Capacitance per unit area (C_i) vs. frequency (f), **(B)** dissipation factor (DF) vs. frequency (f), and **(C)** capacitance per unit area (C_i) vs. voltage (V) of the fabricated cashew gum MIM capacitors.

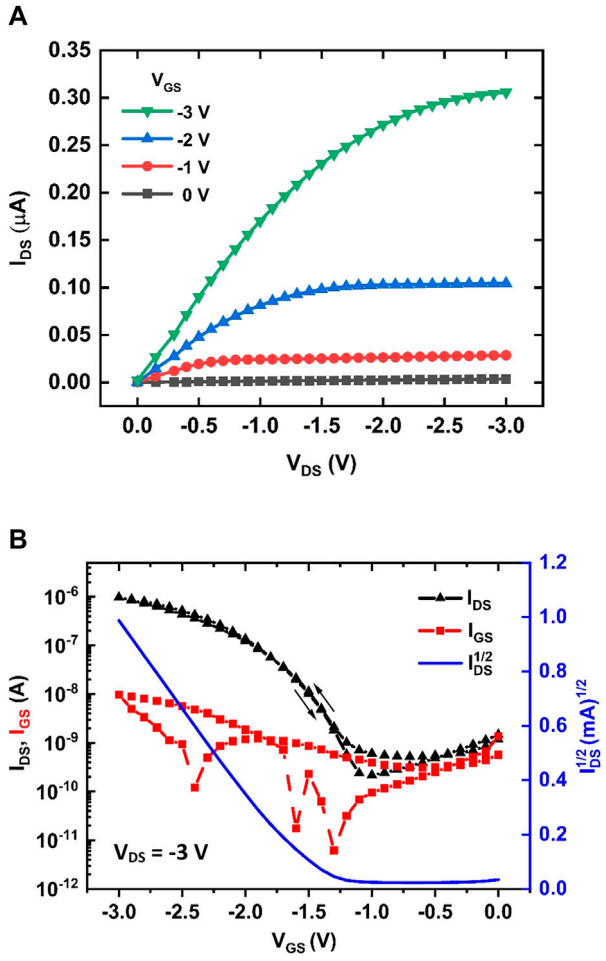

FIGURE 6
Typical **(A)** output and **(B)** transfer characteristics of the fabricated DPPTTT:PMMA OFETs using cashew gum as the gate dielectric. All electrical characterisations were performed in ambient conditions at 23°C and ~40% RH.

39.6 at 100 Hz to 29.3 at 1 MHz. The calculated value of k is much higher than k of the high dielectric constant polymers such as cyanoethyl pullulan (k = 15–21) but somewhat smaller than k of poly(vinylidene fluoride)-based terpolymers (k > 40), and indeed similar to the previously reported dielectric constant of CG (Gadinski et al., 2015; Ramesan and Surya, 2016; Yi et al., 2021). The DF of the studied capacitors drops from 0.2 at 100 Hz to 0.1 at 1 kHz, then it is relatively stable from 1 kHz to 100 kHz, and eventually increases to about 0.4 at 1 MHz. Preferably, for a given capacitor DF should be close to zero. As shown in Figure 5B, the cashew gum capacitors display DF > 0 at all studied frequencies which is not ideal. However, similar DF results are observed in most of naturally occurring and synthetic polymers containing polar moieties (Yu et al., 2008; Wang et al., 2022). The effect of the applied voltage on the measured capacitance at f = 1 kHz is depicted in Figure 5C. As can be seen, the capacitance per unit area C_i remains constant when the applied voltage V varies between −4 and 4 V. Such stable electric behaviour of C_i vs. V is highly desired because it guarantees the reliable operation of electronic devices (Cai et al., 2019; Seck et al., 2021).

3.3 Characterization of cashew gum based OFETs

To test the suitability of cashew gum in OFETs, BGTC transistors using pristine DPPTTT were fabricated.

TABLE 3 Parameters of the fabricated DPPTTT:PMMA OFETs using cashew gum as the gate dielectric compared with organic transistors using other biopolymer dielectrics.

Dielectric	μ_{SAT} (cm^2/Vs.)	V_{th} (V)	$I_{ON/OFF}$	SS (mV/dec)	Active layer	Reference
Silver fir resin +18 nm Al_2O_3	0.04	−1.00	~10^3	1,200	pentacene	Ivić et al. (2022)
Rocky mountain fir +18 nm Al_2O_3	0.04	−0.30	~10^3	600	pentacene	Ivić et al. (2022)
Kraft lignin +18 nm Al_2O_3	0.01	—	~10^3	—	C_{60}	D'Orsi et al. (2022)
Kraft lignin +18 nm Al_2O_3	0.07	—	~10^3	—	pentacene	D'Orsi et al. (2022)
Almond gum	0.75	−0.80	> 10^3	266	DPPTTT:PMMA	Seck et al. (2020a)
Gum arabic	0.60	−0.35	> 10^2	350	DPPTTT:PMMA	Seck et al. (2020b)
Khaya gum	0.30	−1.30	> 10^3	450	DPPTTT:PMMA	Tall et al. (2022)
Glucose	0.09	—	~10^4	6,200	C_{60}	Irimia-Vladu et al. (2010b)
Guanine	0.12	—	~10^3	1,400	C_{60}	Irimia-Vladu et al. (2010b)
Cytosine	0.09	—	~10^3	1,200	C_{60}	Irimia-Vladu et al. (2010b)
Lactose	0.05	—	~10^4	2000	C_{60}	Irimia-Vladu et al. (2010b)
Silk fibroin	10	+5.90	10^3	<500	C_{60}/pentacene	Tsai et al. (2013)
Chicken albumen	0.09	−8.00	10^4	<2000	pentacene	Chang et al. (2011)
Gum arabic +14 nm Al_2O_3	0.56	−2.60	~10^3	140	pentacene	Stadlober et al. (2015)
Gum mastic +14 nm Al_2O_3	0.02	−3.00	~10^3	240	pentacene	Stadlober et al. (2015)
Cashew gum	0.20	−1.40	> 10^3	250	DPPTTT:PMMA	This work

Unfortunately, none of the fabricated devices operated as expected because of the relatively high leakage current (I_G) through the gate dielectric that was comparable with or higher than the drain-source current (I_{DS}). Therefore, DPPTTT:PMMA polymer binary blend with a solution volume ratio of 7:3 was used as the active material. The representative output and transfer characteristics of the engineered DPPTTT:PMMA OFETs are illustrated in Figures 6A, B, respectively. All parameters of the fabricated transistors were calculated in the saturation regime from their transfer characteristics and are displayed in Table 3. As shown in Figure 6A, the devices operate in the accumulation mode and show a typical p-channel transistor behaviour with well-defined linear and saturation regimes. The field-effect mobility in the saturation regime calculated using the standard MOSFET equation is found to be μ_{sat} = (0.20 ± 0.05) cm^2/Vs. (Horowitz, 1998) This value is somewhat lower than that of the DPPTTT:PMMA OFETs using other natural gums as the gate dielectric but higher than, for example, μ_{sat} of the recently reported pentacene FETs using fir resins or kraft lignin as the gate dielectric (cf. Table 3). (Ivić et al., 2022; D'Orsi et al., 2022) As can be seen in Figure 6B, the fabricated transistors display a negligible current-voltage hysteresis during the forward and backward gate voltage sweeps. The hysteresis is often attributed to the charge-trapping phenomenon in the semiconductor layer, gate dielectric and/or at the semiconductor-dielectric interface, and should be as small as possible (Lee et al., 2014). The subthreshold swing is calculated to be SS = (250 ± 10) mV/dec which is comparable with the previously reported SS values for low-voltage organic FETs using polymer semiconductors (Duan et al., 2020; Amna et al., 2022). It is worth noting that in organic transistors charge transport occurs in the first few monolayers of the semiconductor. As a result, to achieve the best possible device performance, a high-quality dielectric/semiconductor interface with as few as possible interfacial states that act as charge carrier traps is required. To quantitatively evaluate the quality of the semiconductor/dielectric interface of the fabricated transistors, the interface trap density (N_{it}) was estimated. To calculate N_{it}, the following equation was used:

$$N_{it} = \left(\frac{SS\log e}{kT/q} - 1\right)\frac{C_i}{q^2} \quad \text{(eq.1)}$$

where *SS* is the subthreshold swing, *e* is the base of the natural logarithm, *k* is the Boltzmann's constant, *T* is the temperature, C_i is the capacitance per unit area, and *q* is the electron charge. (McDowell et al., 2006; Sze and Ng, 2006; Kalb and Batlogg, 2010) It has been found that N_{it} is 5.2 × 10^{12} cm^2/eV that is comparable with previously reported OFETs and almost identical to the N_{it} of the DPPTTT:PMMA OFETs using anodized Ta_2O_5 as the gate dielectric. (Mohammadian et al., 2019) As such, we hypothesise that the vertical phase separation in which the semiconducting DPPTTT layer is on the top and the insulating PMMA layer at the bottom also occurs here. In addition, the amount of PMMA in the used blend is much smaller than DPPTTT which suggests that PMMA forms a thin but robust "buffer layer" between the gate dielectric and the active layer. (Qiu et al., 2008; Lee and Park, 2014) The relatively low threshold voltage of V_{th} = -(1.4 ± 0.1) V and ON/OFF current ratios $I_{ON/OFF} \geq 10^3$ are acceptable for the realization of low-voltage OFET sensors and simple circuits. (Martínez Hardigree and Katz, 2014) Much higher $I_{ON/OFF}$ are usually needed for other transistor applications. The relatively small $I_{ON/OFF}$ of the presented transistors is due to the three orders of magnitude lower I_{ON} and much higher I_{OFF} when

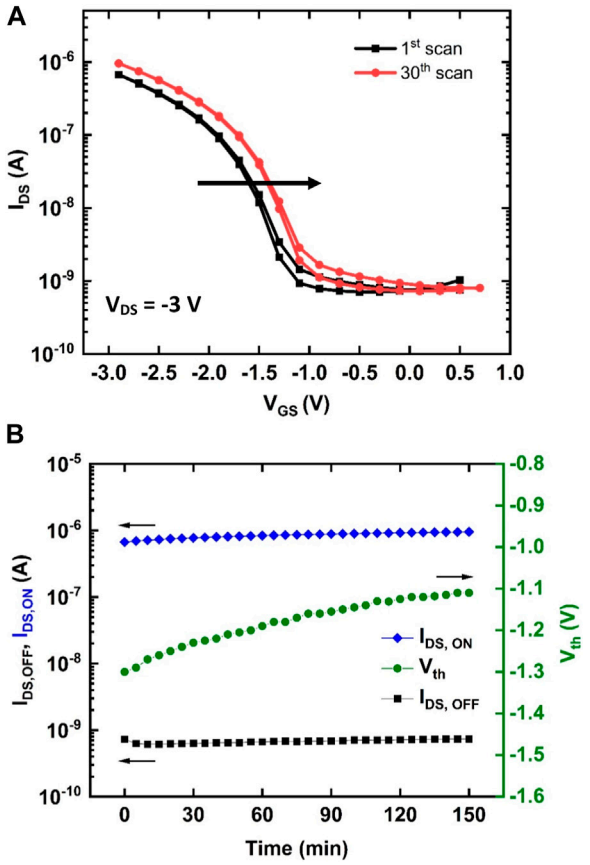

FIGURE 7
(A) Representative transfer characteristics of the fabricated DPPTTT:PMMA OFETs using cashew gum as the gate dielectric before (first scan) and after 150 min (30th scan) of bias stress. **(B)** The evolution of the ON source-drain current ($I_{DS,ON}$), OFF source-drain current ($I_{DS,OFF}$), and threshold voltage (V_{th}) during BS. All electrical characterisations were performed in ambient conditions at 23°C and ~40% RH.

compared with the high ON/OFF current ratio pentacene transistors ($I_{ON/OFF} \geq 10^7$). (Müller et al., 2011) Whereas the much lower field-effect mobility is the possible reason for the significantly reduced I_{ON} the much higher I_{OFF} is most likely caused by the leakage current through the gate insulator and unintentional doping of DPPTTT. As revealed in Figure 6B, the leakage current through the gate dielectric (I_G) reaches 10^{-8} A at V_{GS} = −3 V. Since I_{OFF} current is a combination of the gate leakage and bulk currents in the semiconductor, high I_G quickly leads to the degradation of the $I_{ON/OFF}$ and rapid increase of the static power dissipation. One possible way to decrease I_G and increase the $I_{ON/OFF}$ current ratio in the reported DPPTTT:PMMA OFETs is to shrink the device dimensions and pattern the active layer. However, more research is needed to confirm that this approach indeed improves the performance of the researched devices.

3.4 Evaluation of OFET bias stress

In order to assess the electrical instability of the fabricated DPPTTT:PMMA OFETs during operation, bias stress (BS) measurements were performed. Figure 7A shows typical transfer characteristics of the tested OFETs before (first scan) and after 150 min (30th scan) of BS. The time interval between each measurement was 5 min. The full set of the measured transfer curves is shown in Supplementary Figure S1. As can be seen, only a small positive shift of the I_{DS} vs. V_{GS} characteristics occurs. As displayed in Figure 7B, while the "on" source-drain current ($I_{DS,ON}$) measured at V_{GS} = −3 V slightly increases from 0.7 to 0.9 μA, the "off" source-drain current ($I_{DS,OFF}$) recorded at V_{GS} = 0 V stays almost unchanged at about 0.5 nA during the designated stress time. The observed small positive shift of the threshold voltage ($|\Delta V_{th}|$ = 0.2 V) is likely due to an increased fraction of deeply trapped charge carriers that no longer contribute to charge transport (Simatos et al., 2021). Intriguingly, it appears that DPPTTT:PMMA OFETs using cashew gum as the gate insulator are more electrically stable than the organic transistors using khaya gum (Tall et al., 2022). However, BS in OFETs is still not well understood and it remains unclear what exactly causes this phenomenon in devices. It is believed that migration of mobile ions and charge trapping taking place in the gate dielectric, at the semiconductor/dielectric interface, and within the semiconductor active layer may also be responsible for the observed $I_{DS,ON}$ change and the V_{th} shift (Rep et al., 2003; Gomes et al., 2004; Liu et al., 2015). Intriguingly, the strength of BS is strongly dependent on the involved materials, the device geometry, as well as the transistor polarization conditions and the atmosphere in which the OFET is operated. Although further intensive optimization works are needed to improve the operation of the demonstrated transistors, the devices appear to perform sufficiently well for many practical applications.

4 Conclusion

In this work, OFETs using DPPTTT:PMMA semiconductor-insulator blend as the active layer and cashew gum as the gate dielectric operating with the gate voltages $|V_{GS}| \leq 3$ V are demonstrated. The XRD studies of the prepared cashew gum powder reveal that the biopolymer is largely amorphous. The EDXRF analysis shows that the material contains major mineral elements represented as their corresponding oxides and other mineral chemical elements in trace. The prepared cashew gum films appear to be relatively rough with an RMS roughness of around 1.2 nm and a PTV distance of about 10.2 nm. The surface of the gum is hydrophilic. The areal capacitance at 1 kHz obtained from the electrical characterization of the fabricated MIM capacitors is found to be (260 ± 28) nF/cm^2 for (130 ± 20) nm thick films. Consequently, the dielectric constant k of the material is calculated to be 38 ± 2. The electrical parameters of the fabricated DPPTTT:PMMA OFETs including the saturation field effect mobility μ_{sat} = (0.20 ± 0.05) cm^2/Vs., threshold voltage V_{th} = -(1.4 ± 0.1) V, subthreshold swing SS = (250 ± 10) mV/dec, and ON/OFF current ratio $I_{ON/OFF} \geq 10^3$ show that well-operating devices can be achieved. As a result, cashew gum emerges as a promising high-k biopolymer for sustainable fabrication of low voltage operated OFETs.

Data availability statement

The raw data supporting the conclusion of this article will be made available by the authors, without undue reservation.

Author contributions

SF: Conceptualization, Data curation, Formal Analysis, Investigation, Methodology, Validation, Visualization, Writing–review and editing, Software, Writing–original draft. AbT: Conceptualization, Formal Analysis, Investigation, Methodology, Visualization, Writing–review and editing. NM: Formal Analysis, Investigation, Methodology, Writing–review and editing. MaS: Formal Analysis, Investigation, Methodology, Writing–review and editing. MeS: Formal Analysis, Writing–review and editing, Investigation, Methodology. AyT: Formal Analysis, Writing–review and editing, Investigation, Methodology. ME: Formal Analysis, Resources, Supervision, Writing–review and editing. KK: Formal Analysis, Resources, Supervision, Writing–review and editing. AD: Conceptualization, Data curation, Formal Analysis, Project administration, Resources, Software, Supervision, Visualization, Writing–original draft, Writing–review and editing. LM: Conceptualization, Data curation, Formal Analysis, Project administration, Resources, Software, Supervision, Visualization, Writing–original draft, Writing–review and editing.

Funding

The author(s) declare that no financial support was received for the research, authorship, and/or publication of this article.

Acknowledgments

AT and AKD would like to thank the Centre d'Excellence Africain en Mathématiques, Informatique et TIC (CEA-MITIC) for financial support. Also, all authors would like to thank A. P. Alloncle for AFM imaging of the samples.

Conflict of interest

The authors declare that the research was conducted in the absence of any commercial or financial relationships that could be construed as a potential conflict of interest.

The author(s) declared that they were an editorial board member of Frontiers, at the time of submission. This had no impact on the peer review process and the final decision.

Publisher's note

Supplementary material

The Supplementary Material for this article can be found online at: https://www.frontiersin.org/articles/10.3389/fmats.2023.1280543/full#supplementary-material

References

Amna, B., Isci, R., Siddiqi, H. M., Majewski, L. A., Faraji, S., and Ozturk, T. (2022). High-performance, low-voltage organic field-effect transistors using thieno[3,2-b] thiophene and benzothiadiazole co-polymers. *J. Mat. Chem. C* 10, 8254–8265. doi:10.1039/D2TC01222G

Bedan, K., Brayant, K., and Mishflo, E. (2014). The effect of soil chemical properties on basic gum composition. *Afr. J. Food Sci. Res.* 2, 115.

Cai, W., Wilson, J., Zhang, J., Park, S., Majewski, L., and Song, A. (2019). Low-voltage, flexible InGaZnO thin-film transistors gated with solution-processed, ultra-thin Al_xO_y. *IEEE Electron Device Lett.* 40, 1. doi:10.1109/LED.2018.2882464

Cenci, M. P., Scarazzato, T., Munchen, D. D., Dartora, P. C., Veit, H. M., Bernardes, A. M., et al. (2022). Eco-friendly electronics - a comprehensive review. *Adv. Mat. Technol.* 7 (2), 2001263. doi:10.1002/admt.202001263

Chang, J.-W., Wang, C.-G., Huang, C.-Y., Tsai, T.-D., Guo, T.-F., and Wen, T.-C. (2011). Chicken albumen dielectrics in organic field-effect transistors. *Adv. Mat.* 23, 4077–4081. doi:10.1002/adma.201102124

Chiong, J. A., Tran, H., Lin, Y., Zheng, Y., and Bao, Z. (2021). Integrating emerging polymer chemistries for the advancement of recyclable, biodegradable, and biocompatible electronics. *Adv. Sci.* 8 (14), 2101233. doi:10.1002/advs.202101233

Dendena, B., and Corsi, S. (2014). Cashew, from seed to market: a review. *Agron. Sustain. Dev.* 34, 753–772. doi:10.1007/s13593-014-0240-7

de Oliveira, E. F., Paula, H. C. B., and de Paula, R. C. M. (2014). Alginate/cashew gum nanoparticles for essential oil encapsulation. *Colloids Surf. B Biointerfaces* 113, 146–151. doi:10.1016/j.colsurfb.2013.08.038

D'Orsi, R., Irimia, C. V., Lucejko, J. J., Kahraman, B., Kanbur, Y., Yumusak, C., et al. (2022). Kraft lignin: from pulping waste to bio-based dielectric polymer for organic field-effect transistors. *Adv. Sustain. Syst.* 6, 2200285. doi:10.1002/adsu.202200285

Duan, Y., Zhang, B., Zou, S., Fang, C., Wang, Q., Shi, Y., et al. (2020). Low-power-consumption organic field-effect transistors. *J. Phys. Mat.* 3, 014009. doi:10.1088/2515-7639/ab6305

Fosu, M.-A., Ofori-Kwakye, K., Kuntworbe, N., and Bonsu, M. A. (2016). Investigation of blends of cashew and xanthan gums as a potential carrier for colonic delivery of Ibuprofen. *Int. J. Pharmtech. Res.* 9, 369.

Gadinski, M. R., Li, Q., Zhang, G., Zhang, X., and Wang, Q. (2015). Understanding of relaxor ferroelectric behavior of poly(vinylidene fluoride–trifluoroethylene–chlorotrifluoroethylene) terpolymers. *Macromolecules* 48, 2731–2739. doi:10.1021/acs.macromol.5b00185

Gomes, H. L., Stallinga, P., Dinelli, F., Murgia, M., Biscarini, F., de Leeuw, D. M., et al. (2004). Bias-induced threshold voltages shifts in thin-film organic transistors. *Appl. Phys. Lett.* 84, 3184–3186. doi:10.1063/1.1713035

Guo, S., Wang, Z., Chen, X., Li, L., Li, J., Ji, D., et al. (2022). Low-voltage polymer-dielectric-based organic field-effect transistors and applications. *Nano Sel.* 3, 20–38. doi:10.1002/nano.202100051

Gyedu-Akoto, E., Oduro, I., Amoah, F. M., Oldham, J. H., Ellis, W. O., and Opoku-Ameyaw, K. (2008). Physico-chemical properties of cashew tree gum. *Afr. J. Food Sci.* 2, 60. doi:10.5897/AJFS.9000229

Hasnain, M. S., and Nayak, A. K. (2019). *Natural polysaccharides in drug delivery and biomedical applications*. Amsterdam, Netherlands: Elsevier. doi:10.1016/C2018-0-01566-2

Horowitz, G. (1998). Organic field-effect transistors. *Adv. Mat.* 10, 365–377. doi:10.1002/(SICI)1521-4095(199803)10:5<365::AID-ADMA365>3.0.CO;2-U

Hu, P., He, X., and Jiang, H. (2021). Greater than 10 $cm^2 V^{-1} s^{-1}$: a breakthrough of organic semiconductors for field-effect transistors. *InfoMat* 3, 613–630. doi:10.1002/inf2.12188

Irimia-Vladu, M. (2014). Green' electronics: biodegradable and biocompatible materials and devices for sustainable future. *Chem. Soc. Rev.* 43 (2), 588–610. doi:10.1039/C3CS60235D

Irimia-Vladu, M., Troshin, P. A., Reisinger, M., Schwabegger, G., Ullah, M., Schwoediauer, R., et al. (2010b). Environmentally sustainable organic field effect transistors. *Org. Electron.* 11, 1974–1990. doi:10.1016/j.orgel.2010.09.007

Irimia-Vladu, M., Troshin, P. A., Reisinger, M., Shmygleva, L., Kanbur, Y., Schwabegger, G., et al. (2010a). Biocompatible and biodegradable materials for organic field effect transistors. *Adv. Funct. Mat.* 20, 4069–4076. doi:10.1002/adfm.201001031

Ivić, J., Petritz, A., Irimia, C. V., Kahraman, B., Kanbur, Y., Bednorz, M., et al. (2022). Pinaceae fir resins as natural dielectrics for low voltage operating, hysteresis-free organic field effect transistors. *Adv. Sustain. Syst.* 6, 2200234. doi:10.1002/adsu.202200234

Kalb, W. L., and Batlogg, B. (2010). Calculating the trap density of states in organic field-effect transistors from experiment: a comparison of different methods. *Phys. Rev. B* 81, 035327. doi:10.1103/PhysRevB.81.035327

Kim, M. P., Ahn, C. W., Lee, Y., Kim, K., Park, J., and Ko, H. (2021). Interfacial polarization-induced high-k polymer dielectric film for high-performance triboelectric devices. *Nano Energy* 82, 105697. doi:10.1016/j.nanoen.2020.105697

Lee, E. K., Kim, J. Y., Chung, J. W., Lee, B.-L., and Kang, Y. (2014). Photo-crosslinkable polymer gate dielectrics for hysteresis-free organic field-effect transistors with high solvent resistance. *J. Mat. Chem. C* 4, 293–300. doi:10.1039/C3RA43890B

Lee, W. H., and Park, Y. D. (2014). Organic semiconductor/insulator polymer blends for high-performance organic transistors. *Polymers* 6, 1057–1073. doi:10.3390/polym6041057

Liu, Y., Diallo, A. K., and Katz, H. E. (2015). Ion polarization behavior in alumina under pulsed gate bias stress. *Appl. Phys. Lett.* 106, 112906. doi:10.1063/1.4916227

Majewski, L. A., Schroeder, R., and Grell, M. (2004). Organic field-effect transistors with ultrathin gate insulator. *Synth. Mater.* 144, 97–100. doi:10.1016/j.synthmet.2004.02.012

Martínez Hardigree, J. F., and Katz, H. E. (2014). Through thick and thin: tuning the threshold voltage in organic field-effect transistors. *Acc. Chem. Res.* 47, 1369–1377. doi:10.1021/ar5000049

McDowell, M., Hill, I. G., McDermott, J. E., Bernasek, S. L., and Schwartz, J. (2006). Improved organic thin-film transistor performance using novel self-assembled monolayers. *Appl. Phys. Lett.* 88, 073505. doi:10.1063/1.2173711

Mohammadian, N., Faraji, S., Sagar, S., Das, B. C., Turner, M. L., and Majewski, L. A. (2019). One-volt, solution-processed organic transistors with self-assembled monolayer-Ta_2O_5 gate dielectrics. *Materials* 12 (16), 2563. doi:10.3390/ma12162563

Müller, R., Smout, S., Rolin, C., Genoe, J., and Heremans, P. (2011). High mobility short-channel p-type organic transistors with reduced gold content and completely gold-free source/drain bottom contacts. *Org. Electron.* 12, 1227–1235. doi:10.1016/j.orgel.2011.03.033

H. N. Murthy (Editor) (2022). *"Gums, resigns, and latexes of plant origin - chemistry, biological activities and uses"* (Switzerland: Springer Nature Switzerland AG). doi:10.1007/978-3-030-91378-6

Nketia-Yawson, B., and Noh, Y.-Y. (2018). Recent progress on high-capacitance polymer gate dielectrics for flexible low-voltage transistors. *Adv. Funct. Mat.* 28 (42), 1802201. doi:10.1002/adfm.201802201

Oliveira, A. C. de J., Chaves, L. L., Ribeiro, F. d. O. S., de Lima, L. R. M., Oliveira, T. C., García-Villén, F., et al. (2021). Microwave-initiated rapid synthesis of phthalated cashew gum for drug delivery systems. *Carbohydr. Polym.* 254, 117226. doi:10.1016/j.carbpol.2020.117226

Paterson, A. F., Mottram, A. D., Faber, H., Niazi, M. R., Fei, Z., Heeney, M., et al. (2019). Impact of the gate dielectric on contact resistance in high-mobility organic transistors. *Adv. Electron. Mat.* 5, 1800723. doi:10.1002/aelm.201800723

Phillips, G. O., and Williams, P. A. (2020). *Handbook of hydrocolloids*. 2nd Edition. Sawston: Woodhead Publishing. doi:10.1016/C2018-0-04245-0

Qiu, L., Lim, J. A., Wang, X., Lee, W. H., Hwang, M., and Cho, K. (2008). Versatile use of vertical-phase-separation-induced bilayer structures in organic thin-film transistors. *Adv. Mat.* 20, 1141–1145. doi:10.1002/adma.200702505

Ramesan, M. T., and Surya, K. (2016). Studies on electrical, thermal and corrosion behaviour of cashew tree gum grafted poly(acrylamide). *Polym. Renew. Resour.* 7, 81–99. doi:10.1177/204124791600700302

Rep, D. B. A., Morpurgo, A. F., Sloof, W. G., and Klapwijk, T. M. (2003). Mobile ionic impurities in organic semiconductors. *J. Appl. Phys.* 93, 2082–2090. doi:10.1063/1.1538338

Rezaei, A., Tavanai, H., and Nasirpour, A. (2016). Fabrication of electrospun almond gum/PVA nanofibers as a thermostable delivery system for vanillin. *Int. J. Biol. Macromol.* 91, 536–543. doi:10.1016/j.ijbiomac.2016.06.005

Ribeirod, A. J., de Souza, F. R. L., Bezerra, J. M., Oliveira, C., Nadvorny, D., de La Roca Soares, M. F., et al. (2016). Gums' based delivery systems: review on cashew gum and its derivatives. *Carbohydr. Polym.* 147, 188–200. doi:10.1016/j.carbpol.2016.02.042

Seck, M., Diallo, A. K., Erouel, M., Saadi, M., Tiss, B., Wederni, M. A., et al. (2021). Dielectric investigation and material properties of almond gum thin films deposited by spray pyrolysis. *Mat. Chem. Phys.* 272, 124917. doi:10.1016/j.matchemphys.2021.124917

Seck, M., Mohammadian, N., Diallo, A. K., Faraji, S., Erouel, M., Bouguila, N., et al. (2020a). Organic FETs using biodegradable almond gum as gate dielectric: a promising way towards green electronics. *Org. Electron.* 83, 105735. doi:10.1016/j.orgel.2020.105735

Seck, M., Mohammadian, N., Diallo, A. K., Faraji, S., Saadi, M., Erouel, M., et al. (2020b). Low voltage organic transistors with water-processed gum Arabic dielectric. *Synth. Mater.* 267, 116447. doi:10.1016/j.synthmet.2020.116447

Seong, H., Baek, J., Pak, K., and Im, S. G. (2015). A surface tailoring method of ultrathin polymer gate dielectrics for organic transistors: improved device performance and the thermal stability thereof. *Adv. Funct. Mat.* 25, 4462–4469. doi:10.1002/adfm.201500952

Simatos, D., Spalek, L. J., Kraft, U., Nikolka, M., Jiao, X., McNeill, C. R., et al. (2021). The effect of the dielectric end groups on the positive bias stress stability of N2200 organic field effect transistors. *Apl. Mater.* 9, 041113. doi:10.1063/5.0044785

Stadlober, B., Karner, E., Petritz, A., Fian, A., and Irimia-Vladu, M. (2015). Nature as microelectronic fab: bioelectronics: Materials, transistors and circuits. *45th Eur. Solid State Device Res. Conf. (ESSDERC)* 10. doi:10.1109/ESSDERC.2015.7324701

Sze, S. M., and Ng, K. K. (2006). *Physics of semiconductor devices*. Hoboken, New Jersey: John Wiley & Sons, Inc. doi:10.1002/0470068329

Tall, A., Faraji, S., Diallo, A. K., Mohammadian, N., Erouel, M., Seck, M., et al. (2022). Khaya gum – a natural and eco-friendly biopolymer dielectric for low-cost organic field-effect transistors (OFETs). *J. Mater. Sci. Mater. Electron.* 33, 15283–15295. doi:10.1007/s10854-022-08388-2

Tretinnikov, O. N., and Ikada, Y. (1994). Dynamic wetting and contact angle hysteresis of polymer surfaces studied with the modified Wilhelmy balance method. *Langmuir* 10, 1606–1614. doi:10.1021/la00017a047

Tsai, L.-S., Hwang, J.-C., Lee, C.-Y., Lin, Y.-T., Tsai, C.-L., Chang, T.-H., et al. (2013). Solution-based silk fibroin dielectric in n-type C_{60} organic field-effect transistors: mobility enhancement by the pentacene interlayer. *J. Appl. Phys. Lett.* 103, 233304. doi:10.1063/1.4841595

Urasinska-Wojcik, B., Cocherel, N., Wilson, R., Burroughes, J., Opoku, J., Turner, M. L., et al. (2015). 1 Volt organic transistors with mixed self-assembled monolayer/Al_2O_3 gate dielectrics. *Org. Electron.* 26, 20–24. doi:10.1016/j.orgel.2015.07.009

Vázquez-González, Y., Prieto, C., Filizoglu, M., Ragazzo-Sánchez, J., Calderón-Santoyo, M., Furtado, R., et al. (2021). Electrosprayed cashew gum microparticles for the encapsulation of highly sensitive bioactive materials. *Carbohydr. Polym.* 264, 118060. doi:10.1016/j.carbpol.2021.118060

Wang, S., Yang, C., Li, X., Jia, H., Liu, S., Liu, X., et al. (2022). Polymer-based dielectrics with high permittivity and low dielectric loss for flexible electronics. *J. Mat. Chem. C* 10, 6196–6221. doi:10.1039/D2TC00193D

Wang, Y., Huang, X., Li, T., Li, L., Guo, X., and Jiang, P. (2019). Polymer-based gate dielectrics for organic field-effect transistors. *Chem. Mat.* 31 (7), 2212–2240. doi:10.1021/acs.chemmater.8b03904

Xia, W., and Zhang, Z. (2018). PVDF-based dielectric polymers and their applications in electronic materials. *IET Nanodielectrics* 1, 17–31. doi:10.1049/iet-nde.2018.0001

Xu, T., Liu, Y., Bu, Y., Shu, S., Fan, S., Cao, M., et al. (2023). Newly synthesized high-k polymeric dielectrics with cyclic carbonate functionality for highly stability organic field-effect transistor applications. *Adv. Electron. Mat.* 9 (1), 2200984. doi:10.1002/aelm.202200984

Yi, K., Liu, J., Chen, P., and Chu, B. (2021). Miscibility, microstructure, and dielectric properties of the polymer blends of cyanoethyl pullulan and fluoroterpolymer. *J. Mater. Sci. Mater. Electron.* 32, 3577–3590. doi:10.1007/s10854-020-05104-w

Yu, X., Yi, B., Liu, F., and Wang, X. (2008). Prediction of the dielectric dissipation factor tanδ of polymers with an ANN model based on the DFT calculation. *React. Funct. Polym.* 68, 1557–1562. doi:10.1016/j.reactfunctpolym.2008.08.009